UNIVERSITI PUTRA MALAYSIA

DIELECTRIC AND OPTICAL PROPERTIES OF LEAD-BOROTELLURITE GLASS SYSTEM

ISKANDAR SHAHRIM MUSTAFA

FS 2011 37

DIELECTRIC AND OPTICAL PROPERTIES OF LEAD-BOROTELLURITE GLASS SYSTEM

By

ISKANDAR SHAHRIM MUSTAFA

Thesis Submitted to the School of Graduate Studies, Universiti Putra Malaysia, in Fulfilment of the Requirement for the Degree of Doctor of Philosophy

July 2011

To:

My beloved mom, Siti Ishah bt Md. Hanafi

and

My lovely wife, Aida Halila binti Ismail

Thanks for the encouragement, love and support in fulfilling my endeavour...

Abstract of thesis presented to the Senate of Universiti Putra Malaysia in fulfilment of the requirement for the degree of Doctor of Philosophy

DIELECTRIC AND OPTICAL PROPERTIES OF LEAD-BOROTELLURITE GLASS SYSTEM

By

ISKANDAR SHAHRIM MUSTAFA

July 2011

Chairman : Halimah binti Mohamed Kamari, PhD

Faculty : Faculty of Science

Homogeneous ternary $(TeO_2)_y$ $[(PbO)_x$ $(B_2O_3)_{1-x}]_{1-y}$ glass system (x = 0.0 - 0.50 and y = 0.7) were successfully synthesized using a conventional melt-quenching method. The glasses were then irradiated at different doses from 5 kGy up to 25 kGy with intervals of 5 kGy with 1.33-MeV gamma rays at a constant dose rate of 3.167 kGy/hours produced by ^{60}Co radionuclide. The effect of dose variation and composition of PbO on the dielectric, optical, physical and structural properties of the $PbO\text{-}B_2O_3\text{-}TeO_2$ glass has been studied. Generally, the increase in the density is related to the high dense PbO (9350 kg/m^3) compared to that of TeO_2 (5670 kg/m^3). This change in density by the addition of PbO is also related to the change in the atomic mass and atomic volume of constituent elements. Furthermore, the observed increase in density of $TeO_2\text{-}PbO\text{-}B_2O_3$ glasses as irradiated with gamma ray is due to a tightening effect or compaction of the glass structure. The XRD diffractograms shows that all the glasses prepared are partially crystalline as the

amount of PbO increased in the glass network. Furthermore, all the glass prepared proved to fit amorphous state as the irradiation dose increases.

The addition of heavy metal oxide modifiers to pure TeO_2 leads to the progressive formation of distorted TeO_{3+1} polyhedron followed by the creation of regular trigonal TeO_3 pyramids that contain non-bridging oxygen. PbO stands out as unique substance because of its dual role (i) as modifier, if Pb-O is ionic (ii) as glass former with PbO_4 structural units, if Pb-O is covalent. Based on the Raman spectra results, the increase broad shoulders at 410 cm^{-1} indicate that new features to vibrations of one of the partially crystalline phase of Pb_3TeO_6. The existence of Pb_3TeO_6 is confirmed by X-ray analysis. The change in T_g indicates a change related to the manner in which PbO gets arranged in the glass. Eventually, the decrease in the glass transition temperature implies a decrease in the rigidity of the network due to addition amount of network intermediate PbO. The glass transition temperature increases with increasing of radiation dose which designate changes of the glass structure.

The optical absorption spectra of the glasses were measured and the Urbach rule has been applied to evaluate the fundamental absorption edges for all the glasses from the obtained spectrum. The optical band gaps were calculated from the absorption edge and it was found that the optical band gap energy, E_{opt} depended on the glass composition and irradiation exposure. The dielectric permittivity is known as the polarizability of the material under external electric field whiles the dielectric loss is contributed to the energy loss during polarization process. The results of dielectric response measurements show that electrode polarization at

low frequency, orientation polarization at intermediate frequency and polarization of defect glass structure at high frequency are the most probable process responsible for the observed dielectric behaviour of the studied glass samples. The peaks are also clearly observed within the imaginary part of the electrical modulus, M'' as a function of frequency at different temperature. Activation energy are observed to decrease with simultaneous successive increase in PbO concentration of $(TeO_2)_y$ $[(PbO)_x$ $(B_2O_3)_{1-x}]_{1-y}$ glasses and irradiation dose. The reasons for such changes may be due to gradual increase in the fraction of octahedrally positioned lead ions in the glass network which act as modifiers. These ions weaken the glass network and create pathways suitable for migration of free ions that build up space charge. Thus, the weaker the network, the more is the space charge polarization, leading to an increase in the dielectric parameters. The phenomenon is supported by (i) decrease in the glass transition temperature T_g and related parameters with PbO concentration, (ii) the splitting of Te-O-Te and B-O-B bonds in the Raman spectra and (iii) decrease in the value of optical band gap, E_{opt}.

Abstrak tesis yang dikemukakan kepada Senat Universiti Putra Malaysia sebagai memenuhi keperluan untuk ijazah Doktor Faksafah.

PENCIRIAN DIELEKTRIK DAN OPTIK SISTEM KACA PLUMBUM-BOROTELLURIT

Oleh

ISKANDAR SHAHRIM MUSTAFA

Julai 2011

Pengerusi : Halimah binti Mohamed Kamari, PhD

Fakulti : Fakulti Sains

Sistem kaca pertigaan homogen $(TeO_2)_y$ $[(PbO)_x$ $(B_2O_3)_{1-x}]_{1-y}$ (x = 0.0 - 0.50 dan y = 0.7) telah disentesiskan dengan jayanya mengunakan kaedah konvensional sepuh lindapan. Kaca itu kemudiannya diradiasikan pada dos berbeza dari 5 kGy hingga 25 kGy dengan sela 5 kGy dengan 1.33-MeV sinar gama pada kadar dos malar 3.167 kGy/jam dihasilkan oleh radionuklid ^{60}Co. Kesan dos radiasi dan komposisi PbO pada pencirian dielektrik, optik, fizikal dan struktur kaca the PbO-B_2O_3-TeO_2 telah dikaji. Keseluruhannya, penigkatan ketumpatan berkait dengan tumpat tinggi PbO (9350 kg/m^3) berbanding terhadap TeO_2 (5570 kg/m^3). Perubahan ketumpatan ini dengan pertambahan PbO juga berkait dengan perubahan di dalam jisim atom dan isipadu unsur juzuk atom. Tambahan pula, pencerapan peningkatan ketumpatan kaca PbO-B_2O_3-TeO_2 yang disinarkan dengan sinar gama adalah disebabkan oleh kesan tautan atau pemadatan struktur kaca. Difraktogram XRD menunjukkan yang kesemua kaca yang disediakan adalah separa berhablur apabila bilangan PbO meningkat di dalam rangkaian kaca.

Tambahan pula, kesemua kaca yang disediakan terbukti sepadan keadaan amorfus apabila dos radiasi bertambah.

Pertambahan penguahsuai oksida logam berat terhadap TeO_2 membawa kepada pembentukan progresif terherot poliherdon TeO_{3+1} diikuti dengan penciptaan tetap piramid trigonal TeO_3 yang mengandungi oksigen tak bersambungan. PbO menonjol sebagai bahan unik disebabkan oleh peranan duaan (i) sebagai pengubahsuai, jika Pb-O adalah ionik (ii) sebagai pembentuk kaca dengan struktur unit PbO_4, jika PbO adalah kovalen. Berdasarkan keputusan spektrum Raman, peningkatan bahuan lebar pada 410 cm^{-1} menunjukkan ciri-ciri baru terhadap getaran sebahagian fasa separa berhablur Pb_3TeO_6. Kewujudan Pb_3TeO_6 disahkan dengan analisis sinar-X. Perubahan T_g menunjukkan perubahan berkait dengan cara di mana PbO disusun di dalam kaca. Keseluruhannya, pengurangan suhu peralihan kaca menandakan pengurangan di dalam ketegaran rangkaian akibat daripada pertambahan pengantara rangkaian PbO. Suhu peralihan kaca bertambah dengan pertambahan dos radiasi yang menandakan perubahan struktur kaca.

Spektrum penyerapan optik kaca telah diukur dan peraturan Urbach telah digunapakai untuk menilai asasi penyerapan pinggiran untuk kesemua kaca daripada spektrum yang diperolehi. Sela jalur optik telah dihitung daripada penyerapan pinggiran dan didapati tenaga sela jalur optik, E_{opt} bergantung terhadap komposisi kaca serta pendedahan penyinaran. Ketelusan dielektrik dikenali sebagai kebolehkutuban sesuatu bahan di bawah medan elektrik luaran sementara kehilangan dielektrik menyumbang kepada kehilangan tenaga semasa proses pengutuban. Keputusan pengukuran sambutan dielektrik menunjukkan

pengutuban elektrod di frekuensi rendah, penghalaan pengutuban di frekuensi sederhana dan pengutuban kecacatan struktur kaca di frekuensi tinggi adalah proses yang berkemungkinan besar bertanggungjawab terhadap cerapan kelakuan dielektrik sampel kaca yang dikaji. Puncak-puncak juga dicerap jelas di dalam bahagian khayalan modulus elektrik, M'' sebagai fungsi frekuensi pada suhu berbeza. Tenaga pengaktifan dicerap berkurangan serentak dengan peningkatan kepekatan PbO kaca $(TeO_2)_y$ $[(PbO)_x$ $(B_2O_3)_{1-x}]_{1-y}$ dan dos penyinaran. Alasan untuk perubahan yang berlaku mungkin disebabkan peningkatan secara beransur di dalam pecahan kedudukan octahedral ion plumbum di dalam rangkaian kaca yang mana bertindak sebagai pengubahsuai. Ion ini melemahkan rangkaian kaca dan membina laluan yang sesuai untuk perpindahan ion bebas yang membina ruangan cas. Justeru, semakin lemah rangkaian, semakin banyak ruang cas pengutuban, menuju ke peningkatan di dalam parameter dielektrik. Fenomena ini disokong oleh (i) pengurangan suhu peralihan kaca T_g dan parameter yang berkait dengan kepekatan PbO, (ii) pemisahan ikatan Te-O-Te dan B-O-B di dalam spektrum Raman dan (iii) pengurangan di dalam nilai sela jalur optik, E_{opt}.

ACKNOWLEDGEMENTS

All the praise and admiration for Allah, the Almighty, Beneficial and the most Merciful, who has enabled me to submit this dissertation.

The authors gratefully would like to acknowledge the following people and organizations for all their advice, help and support, assists, suggestions, motivations and encouragement throughout author's graduate career:

My beloved mother, Siti Ishah Md. Hanafi; my fiancé, Aida Halila Ismail; my supervisor and mentor, Dr. Halimah Mohamed Kamari from Physics Department, Faculty of Science, Universiti Putra Malaysia and co-supervisors; Associate Professor Dr Wan Mohamad Daud Wan Yusoff from Physics Department, Faculty of Science, Universiti Putra Malaysia; Professor Dr. Sidek Hj. Abdul Aziz from Physics Department, Faculty of Science, Universiti Putra Malaysia; Dr. Khairul Zaman Hj. Dahlan from Polymer Technology Division of Malaysia Nuclear Agency (MNA) and staffs. Last but not least my respectful colleagues.

TABLE OF CONTENTS

LIST OF TABLES

LIST OF FIGURES

LIST OF ABBREVIATIONS

γ-ray	Gamma Ray
kGy	kiloGray
IAEA	International Atomic Energy Research
NMR	Nuclear Magnetic Resonance
UV-Vis	Ultraviolet - Visible
N_A	6.022×10^{23} mol^{-1} (Avogadro's number)
BO	Bridging oxygen
NBO	Non-bridging oxygen
K	Kelvin
k	Boltzman constant
T_g	Glass transition temperature
T_c	Crystalline temperature
T_m	Melting temperature
K_H	Hruby's thermal stability parameter $(T_c-T_g)/T_m$.
α	Absorption coefficient
D	Thickness
A	Area
A	Absorbance
E_{opt}	Optical band gap energy
ΔE	Urbach energy
$\hbar\omega$	Photon energy
ε^*	Complex permittivity
ε_0	Free space permittivity

ε'	Dielectric constant
ε''	Dielectric loss factor
ε_s	Static dielectric permittivity
ε_∞	Dielectric permittivity at very high frequency
$\varepsilon(\omega)$	dielectric permittivity as function of angular frequency
τ	Relaxation time (sec)
f_p	Peak frequency
ω_p	Peak angular frequency
ω_c	Characteristic angular frequency
M^*	Complex electrical modulus
M'	Real part of electrical modulus
M''	Imaginary part of electrical modulus
LFD	Low frequency dispersion
DTA	Differential Thermogravimetric Analysis
E_a	Activation energy
ICRU	International Commission on Radiation Units and Measurements

GLOSSARY

This glossary is to define a few words in common use in this thesis. Many other quantities and terms are defined in appropriate locations in the text.

Absorbed dose — Amount of energy deposited by ionizing radiation in a material per unit mass of the material. Usually expresses in the special radiological unit rad or in the SI unit Gray.

Dose (D) — Used broadly for energy deposited in matter from radiation. Units are the rad and the Gray (Gy), which are equivalent, respectively, to ergs/g and 1 J/kg. There, 1rad = 1/100 Gray.

Gamma-ray (γ-ray) — Photon resulting from a transition in an atomic nucleus, either from natural decay of a radioisotope; or from an induced nuclear transition.

Gray — Radiation absorbed dose unit of the Systeme Internationale (SI), of value 1 Jkg^{-1} and equal to 100 rad.

Ionization — Process of removing (or adding) one or more electrons from (or to) an atom or molecule.

Ionizing radiation — Ionizing radiation is the nuclear particles or electromagnetic radiation with sufficient energy to cause ionization of the atoms and molecules composing the material in which the radiation is interacting. Directly ionizing radiations are charged particles that interact directly with the electrons through coulombic interactions. These radiations include, for example alpha particles, beta particles, electrons, and protons. Indirectly ionizing radiations are uncharged radiation (e.g. X-rays, gamma-rays, neutrons) that must interact with the material, producing a charged particle, which then causes further ionization in the material.

Photon — Quantum of electromagnetic radiation. Can be from any region of the electromagnetic spectrum including radio waves and visible light, but in this article referring to quanta in the energy (or wavelength) region of x-rays, gamma-rays, or bremsstrahlung.

CHAPTER 1

INTRODUCTIONS

Tellurite glasses are very promising materials for laser and non- linear application in optics due to some of their important characteristic features such as high refractive index, low phonon maxima and low melting temperature. Furthermore, TeO_2 is known as a conditional glass former, which it is, needs a modifier in order to easily form the glassy state. The formation of glass on two glass formers is of both scientific and practical interest; where the structural network will be perturbed and may lead to the formation of new structural units. Glass forming substances are fall into two categories of either inorganic compounds containing bonds which are partially ionic and partially covalent, or, inorganic or organic compounds which form chain structures with covalent bonds within the chains and van der Waals' bonds between the chains. Amorphous materials such as glasses are widely used in applications from medicine to transport to space flight. Glasses containing heavy metal oxide (HMO) have recently attracted the attention of several researchers for the excellent infrared transmission compared with conventional glasses. The γ-irradiation on glasses is found to affect the optical and physical properties. Hence, radiation damage caused by electrons, alpha particles and gamma rays has been thoroughly investigated. The structural and physical properties of PbO glasses are well described by Worrel and Henshell (El-Moneim, 2002). In previous work, researchers have studied borate glasses containing heavy-metal oxides and shown that it has potential applications in radiation shielding (Khanna *et al.*, 1996).

1.1 Scope of present study

During recent years, there has been an increasing interest in the synthesis, structure and physical properties of heavy metal oxide (HMO) due to their high refractive index, high infrared transparency, high density and increased third-order nonlinear optical susceptibility. The high radiation resistance of the HMO glasses is desirable, since fluorescence decreases significantly with radiation damage (Gopi Sharma *et al.*, 2006, Chen *et al.*, 2001). Gamma and neutron irradiation affect the structure of the glass matrix, resulting in changes in the optical, physical, thermal and electrical properties (Kutub *et al.*, 1996, El-Alaily and Mohamed, 2003, Ezz-Eldin, 1999, Sharma *et al.*, 2006, El Batal, 2007, Balboul, 2008). Apparently, non-silicate glasses such as chalcogenide glasses are significant commercial interest due to their electrical and electronic properties and the transmission of infrared light. Eventually, the stability of tellurium oxides (TeO_2) is one of the properties that originally attracted researchers to study the tellurite glasses. TeO_2 is known as a conditional glass former or network former, which needs a modifier in order to easily form the glassy state. In present work, boron oxide (B_2O_3) has been selected as a network modifier although naturally, B_2O_3 act as a good network former in glass. Addition of B_2O_3 creates a glass with higher melting point and greater ability to withstand temperature changes although it will also attribute the formation of non-bridging oxygen (NBO) in the glass network. Formations of NBO will eventually results decrease of glass rigidity.

In order to produce a practical glass, another compound, known as doping salt is usually added to the glassy substance or rather, the vitreous network, which consist of at least a glass former and a modifier. Doping salt can be classified as

network intermediate. The network intermediate used in present work is lead oxide (PbO). Lead oxide is categorized as network modifier and also glass intermediate. It is usually classified as intermediate because under certain conditions it appears that PbO can join the continuous network, although unable to form networks by itself. PbO may also accommodate interstitially in a glassy network. This means that PbO possibly will act predominantly as glass former at certain mole fractions (Sharma *et al.*, 2006). Addition of PbO reduces the viscosity in tellurite glasses and eventually made the formation of tellurite glasses becoming more fragile and sparkles. Exposure of glasses to high energy radiation usually results in compaction of the glass, with density increases in the order of 1% for very high radiation doses (Shelby, 2005). This compaction occurs at room temperature and is quite stable over long times, with no evidence of room temperature annealing. The density reverts to the pre-irradiation value, however, when the sample is heated, even though the heat treatment temperature may be less than transition glass temperature T_g.

The scope of present work is to study the effect of radiation and glass composition on the temperature stability, physical properties, chemical bonding, optical absorption, dielectric mechanism and the XRD fingerprint of the lead boro-tellurite $(TeO_2)_y$ $[(PbO)_x$ $(B_2O_3)_{1-x}]_{1-y}$ glass system. The major experimental work consists of optical absorbance and dielectric mechanism with respect to temperature, frequency, composition and radiation. Structural studies were not fully included due to unavailability of appropriate equipment to perform the neutron scattering. Moreover to attempt a thorough exploration of all the various

physical properties such as electrical, optical, thermal, radiation, and etcetera would be a very formidable task and virtually impossible considering time limit.

1.2 Problem statement

There are only few evidences published for tellurite glasses containing heavy metal oxide (HMO) as shielding materials. In previous effort, most discussions relates to effect of X-ray, gamma ray and ultra violet irradiation on the optical and structural of borate glasses due to great ability of B_2O_3 as network former to withstand several range of temperature changes besides characterization using ultrasonic speed and elasticity but non relates with TeO_2 as the network former. Basically, only a few literatures focus on the function of PbO in the glass system but there is no meticulous discussion on the PbO abilities as network intermediate, and how it affects the structural, optical and electrical properties of a glass system. All discussions regarding author findings on tellurite glasses as radiation shielding materials will be elaborated in Chapter 2. Occasionally, the glass system of $(TeO_2)_y [(PbO)_x (B_2O_3)_{1-x}]_{1-y}$ in this report is the first ever proposed in the area.

1.3 Objective of research

The main objectives of the present work are summarized as follows:

1. To determine optical band gap and Urbach energy of the lead borotellurite glass system with respect to glass composition and irradiation of γ-ray.
2. To establish the frequency and temperature dependencies of the dielectric response parameters and mechanism with respect to glass compositional and γ-ray irradiation.

3. To ascertain the structural blueprint of the $(TeO_2)_y$ $[(PbO)_x$ $(B_2O_3)_{1-x}]_{1-y}$ glass system and proposed a structural model based on the functional of Raman spectra profile and XRD diffractogram patterns with respect to glass compositional and γ-ray irradiation.

Besides the main objectives, minor study has been done in order to support the above mention main objectives' findings. To achieve this, a systematic study has been performed to understand the variation of irradiation dose as a function PbO composition in borotellurite glasses. The research includes density measurements and analysis as the mainstay in the study of physical properties, differential thermal analysis, and thermal stability analysis.

1.4 Significant of study

Glasses containing heavy metal oxide (HMO) have recently attracted the attention of several researchers for the excellent infrared transmission compared with conventional glasses. Basically, a new material for X-ray shielding has been prepared by author for the usage in radiotherapy and dentistry scanning. Although there are lots of radiation shielding glasses promoted, but most of the glass were deposited with lead on the glass surface which mainly silica glass. Whereas, the tellurite glass system prepared were blend together with PbO as Pb atom is positioned in the interstitial of the glass network.

It is with the greatest intention that the report in this thesis will serve as a significant guiding reference to those considering further research on physical properties of the material. Basically, a new material for X-ray shielding has been

prepared for the usage in radiotherapy and dentistry scanning. Further studies regarding physical, structural, optical and electrical properties have been done in order to commercialize the material in near future. Subsequently, the thickness of the radiation glasses advertised is ≥ 0.8 cm whereas the lead-borotellurite glass prepared is ≤ 0.8 cm.

1.5 Definition of glass

The glasses used by mankind throughout most of the history have been based on silica. Many have thought that silica is a required component of a glass but on contrary human could form an almost limitless number of inorganic glasses which do not contain silica. Glasses are traditionally formed by cooling from a melt. Nevertheless, glass could also be form by vapour deposition, *sol-gel* processing of solutions and neutron irradiation of crystalline materials. Most traditional glasses are inorganic and non-metallic. However, as years passing by, metallic glasses are becoming more common. Obviously, the chemical nature of the material cannot be used to define a glass. All glasses found to date share two common characteristic. Firstly, none of the glass has a long range, periodic atomic arrangement. Secondly, every glass exhibits time-dependant glass transformation behaviour. This behaviour occurs over a temperature range known as the glass transformation region. Thus a glass can be defined as "an amorphous solid completely lacking in long range, periodic atomic structure and exhibiting a region of glass transformation behaviour (Shelby, 2005)." Eventually, any material consists of inorganic, organic, or metallic, formed by any technique, which exhibits glass transformation behaviour, is a glass.

1.6 Glass formation

Consider a small volume of material at high temperature in liquid form at point a on the volume-temperature diagram (V-T diagram) in **Figure 1.1** (Rawson, 1980). On cooling the volume gradually decreases along the path 'abc'. Point 'b' corresponds to T_m, the melting temperature of the corresponding crystal. Melting point is the temperature at which the solid and the liquid have the same vapor pressure. At this temperature, an infinitely small amount of crystals is in thermodynamic equilibrium with the liquid. For a perceptible level of crystallization, some finite amount of undercooling of the liquid to 'a' point 'c' below T_m is required. Cyrstallization occurs if there is sufficiently large number of nuclei present in the mass and a large enough crystal growth rates exists. The location of the point c below T_m varies depending upon when the thermodynamic driving force created by undercooling causes a particular group atom to transform from the liquid state to crystal state. Volume shrinkage accompanies the crystallization. Further cooling, the crystals so formed shrink along the crystal line to the point 'e'.

If the crystallization does not occur below T_m, the liquid mass moves into the supercooled liquid state along the line 'bcf', which is an extrapolation of the line abc. No discontinuities in the V-T. The volume shrinks continuously that is the structure of the liquid rearranges itself into a lower volume along the line 'bcf' required by the lower energy corresponding to a lowered temperature. As cooling continues, the molecules become less and less mobile, that is the viscosity or the system rapidly increases. At sufficient low temperature, the molecular group cannot rearrange themselves fast enough to reach the volume characteristic of that

temperature. The state line then starts a smooth departure from 'bcf' and soon becomes a near-straight line (often roughly parallel to 'de'), ending at point h, when cooled slowly, or at g, when cooled fast. The material in the near straight, low-temperature part of the curve behaves essentially as a solid which is the glassy state.

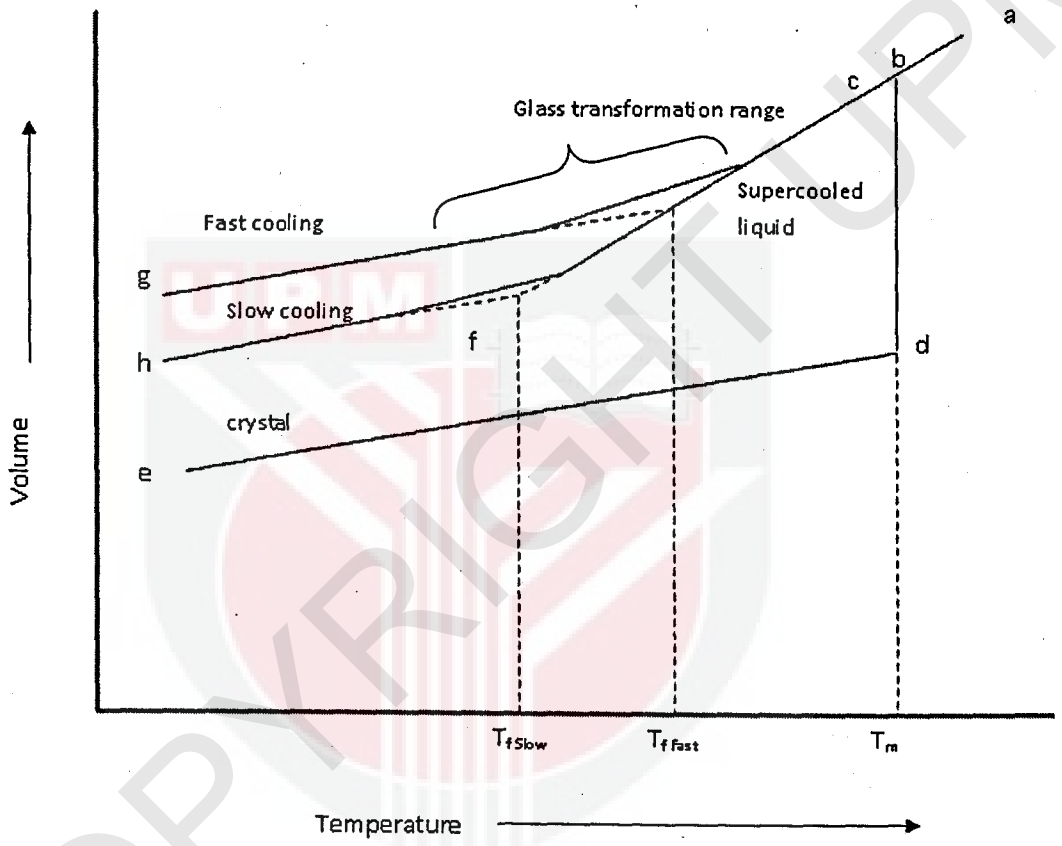

Figure 1.1: The volume-temperature diagram for glass-forming liquid.

The smooth curve between the onset of the departure from the supercooled liquid line and the completion to a seemingly rigid condition is termed the glass transition region, or the glass transformation range. The transition to glassy state does not occur at a single, sharp value of the temperature. In the upper regions, glass has a viscosity of ~ 10^8 Pa.s (equal to 10^9 poise) or less, whereas in the glassy state the viscosity exceeds ~ 10^{15} Pa.s or more to qualify for appearance as

a solid. The intersection of the extrapolated glass line and the supercooled line termed the fictive temperature T_f. Fictive temperature is the temperature at which the structure of the supercooled liquid is instantly frozen into the glass. The departure from the supercooled liquid line is dependent upon the rate of cooling. Slower cooling allows the structure to rearrange itself to stay on 'bcf' longer, and hence the more slowly cooled glass at h would be expected to have a lower volume (higher density) and a lower fictive temperature than a more quickly cooled glass at point 'g'.

1.7 Ionizing radiation

The International Commission on Radiation Units and Measurements (ICRU) has subdivided ionizing radiations into directly and indirectly ionizing radiations based on the different mechanisms by which they interact and lose energy in matter. Directly ionizing radiations are fast charged particles, such as electrons (including beta particles), protons, alpha particles, heavy ions, and charged mesons, which transfer their energy to a bound electron directly and ionize the atom by means of coulomb-force interactions along their track. Indirectly ionizing radiations are uncharged species, such as electromagnetic radiations (X-rays and γ-rays), neutrons, and uncharged mesons, which undergo interactions with matter indirectly releasing secondary charged particles which then take turn to transfer energy directly to a bound electron and ionize the atom. Since this study is concerned with γ-rays, our discussion on radiation interaction with matter is focused on gamma interactions only.

Gamma rays are mono-energetic electromagnetic rays emitted from an excited nucleus. Gamma rays originate from a re-arrangement of nuclear particles (protons and neutrons) and are intended to get rid the excited nuclei of excess energy (Perkins, 1987). The energy and relative intensities of the gamma rays are characteristic to each particular radionuclide. Co-60 radioisotope emits two gamma rays, one at 1.17 MeV and another at 1.33 MeV. Both are emitted at 100% because it is a cascade emission. On average, Cobalt-60 γ-rays have quantum energies of 1.25 MeV. The activity of a radioisotope is governed by a decay law. The activity, A or the rate of decay is proportional to the number of the nuclei N_t present at time t.

$$A = \frac{dN_t}{dt} = -\lambda N \tag{1.1}$$

Integrate Equation (2.1) to obtain a decay law of the activity at time t given by

$$A_t = A_0 e^{-\lambda t} \tag{1.2}$$

The exponential law of decay is characteristic of all radioactive processes and has been checked in vast numbers of experiments over extensive periods. It describes the disappearance by decay of short-lived unstable particles and excited states as well as of long-lived radioactive elements.

1.8 Interaction of gamma ray with matter

Gamma-ray photons are electromagnetic radiations having neither mass nor charge, and interact with atoms of the material irradiated (usually with the orbital electrons from the atoms) by collisions in which energy is transferred from the photon to the atomic particle. The mechanism of photon interactions is defined by absorption and scattering processes. Absorption is characterized by the disappearance of a photon in which the photon energy is taken up by the atom or one of the orbital electrons. Meanwhile, scattering is a combination of absorption and emission of photon. The emission takes place in the new direction with or without a decrease in energy. As a result, atomic excitation will occur by which the innermost orbital electron of the atom has been moved into an outer orbit of higher energy and more distant from the atomic nucleus. On the other hand, an ionisation of the atom occurs when the ejection of the inner orbital electron of the atom by the absorption of photon energy. The ejected electron will then dissipate its energy by further collisions with the other atomic electrons of the materials. Gamma–ray photon can penetrate deeply into matter because of the uncharged elementary particle and lose energy almost entirely through direct collision with the orbital electron. Even atoms of higher atomic number are composed largely of empty space and thus there is a high probability that the incident photon pass through this space without interacting. The number and mode of interactions depend upon the energy of the incident photon and the atomic number of the material (Davisson and Evans, 1952, Roger and Niels, 1970). Moreover, 1.25 MeV gamma-rays emitted from ^{60}Co source can interact with matter in four major mechanisms of photon interaction namely, Rayleigh scattering, photoelectric absorption, Compton scattering, and pair production. The contribution from each

interaction depends on energy of the incident photon and the atomic number of the absorbing medium. All these process lead to the partial or complete transfer of the gamma-ray photon energy to the orbital electron.

1.9 Related theories in experimental results

a. Density and molar volume.

The density is a powerful tool capable of exploring the changes in the structure of glasses. The density is affected by the structural softening/compactness, change in geometrical configuration, coordination number, cross-link density and dimension of interstitial spaces of the glass. The density of a material is defined as the mass of the substance per unit of volume:

$$\rho = \frac{M}{V} \tag{1.3}$$

Where ρ is the density, M is the mass, and V is the volume of the sample. If the sample is free of bubbles, voids or other defects, the calculated density is the true density of the material. If the sample contains bubbles, which occasionally the case for glasses, the calculated density will be less than that of the true density and is termed the apparent density. Inclusion with higher densities than the true density, might be due to particles of unmelted batch or crystal formed during cooling, will cause the apparent density to be greater than the true density. If the available samples do not have simple geometries, Archimedes' principle can be used to determine the volume by liquid displacement. The sample is weighed both in air and suspended in a liquid of known density. The difference in weight equals the weight of the displaced liquid. Since the density of the liquid ρ_L is known, the displaced volume can be calculated using Equation 1.3. Dividing the weight of the

sample in air W_{air}, by the volume of liquid displaced W_L then yields the density of the sample. The density is calculated from the expression (Sidek *et al.*, 2005):

$$\rho_{sample} = \rho_L\left(\frac{W_{air}}{W_L}\right) \tag{1.4}$$

The molar volume is defined as the volume occupied by one mole of a material and is obtained by dividing the molecular weight of a material by its density:

$$V_m = \frac{MW_t}{\rho} \tag{1.5}$$

Where V_m is the molar volume, MW_t is the molecular weight of the substance; ρ is the true density of the material. Since the density of a material is sensitive to both the volume occupied by the atoms and to atomic weight mass, molar volume is often used to compare the behaviour of glasses. In many cases, seemingly anomalous behaviour in density is readily explained by consideration of the molar volume.

1.9.2 X-ray diffraction (XRD)

The principle characteristic of glassy materials is reflected in the short range order and the long range disorder. By disorder, the spatial arrangement of atoms, ions and molecules do not exhibit three dimensional periodicity (translational symmetry), and the long range order of crystalline state is destroyed. The disorder structure of an ideal amorphous state belongs to the topological disorder. Except for some regular arrangement existing in the nearest neighbouring atoms in the bond angle, bond length and coordination number and the arrangements of the next nearest neighbouring atoms are all in disorder. The glass was regarded as amorphous material at an early stage, and that it should have this structure.

Structural information can be obtained by means of X-rays whose wavelengths are less than the spacing among the atoms in the material. Electrons and neutrons encountering the atoms result in interference scattering, and the structure of the order region has been obtained in lots of details with the advancement of X-ray diffraction techniques. Atoms scatter X-ray waves, primarily through the atoms' electrons. Eventually, an X-ray striking an electron produces secondary spherical waves emanating from the electron. This phenomenon is known as elastic scattering, and the electron is known as the *scatterer*. A regular array of scatterers produces a regular array of spherical waves. Although these waves cancel one another out in most directions through destructive interference, they add constructively in a few specific directions, determined by Bragg's law:

$$2dsin\theta = n\lambda \tag{1.6}$$

Here d is the spacing between diffracting planes, θ is the incident angle, n is any integer, and λ is the wavelength of the beam. These specific directions appear as spots on the diffraction pattern called reflections. Thus, X-ray diffraction results from an electromagnetic wave (the X-ray) impinging on a regular array of scatterers.

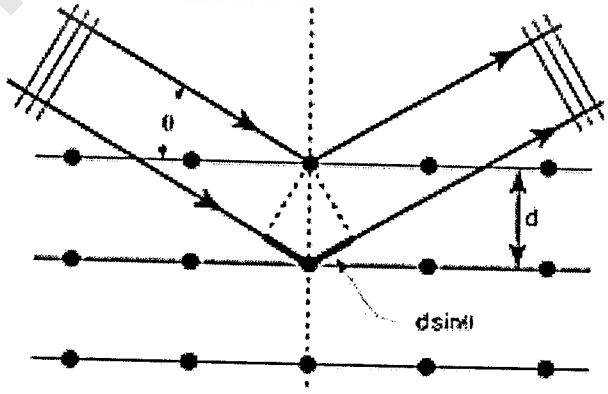

Figures 1.2: X-ray diffraction pattern analysis.

Figures 1.2 shows the incoming beam (coming from upper left) causes each scatterer to re-radiate a small portion of its intensity as a spherical wave. If scatterers are arranged symmetrically with a separation d, these spherical waves will be in sync (add constructively) only in directions where their path-length difference $2d \sin \theta$ equals an integer multiple of the wavelength λ. In that case, part of the incoming beam is deflected by an angle 2θ, producing a reflection spot in the diffraction pattern.

1.9.3 Raman Spectra

The occurrence of Raman scattering may be most easily understood in terms of the quantum theory of radiation. This treats radiation of frequency 'v' as consisting of a stream of particles called photons having energy 'hv' where h is Plank's constant. Photons can be imagined to undergo collisions with molecules and, if the collision is perfectly elastic, it will be deflected unchanged. A detector placed to collect energy at right angles to an incident beam will thus receive photons of energy 'hv', i.e. radiation of frequency 'v'. A photon with the energy $\eta\omega_L$ is incident on the scattering system with the energy level $\eta\omega_R = E_f - E_i$ where i and f are labels of two quantum states.

The Stokes-Raman effect results from the transition from the lower energy level (E_i) to a higher level (E_f). The anti-Stokes effect transfer energy from the system to the incident light wave, which corresponds to the transition from a higher level (E_f) to a lower level (E_i). Since the anti-Stokes scattering occurs from a thermally excited state (E_f), which according to Boltzman statistics is less populated than the

ground state (E_i), the anti-Stokes intensity is less than the Stokes intensity. Hence, in most cases only the Stokes-Raman spectrum is detected (Stephen *et al.*, 1975).

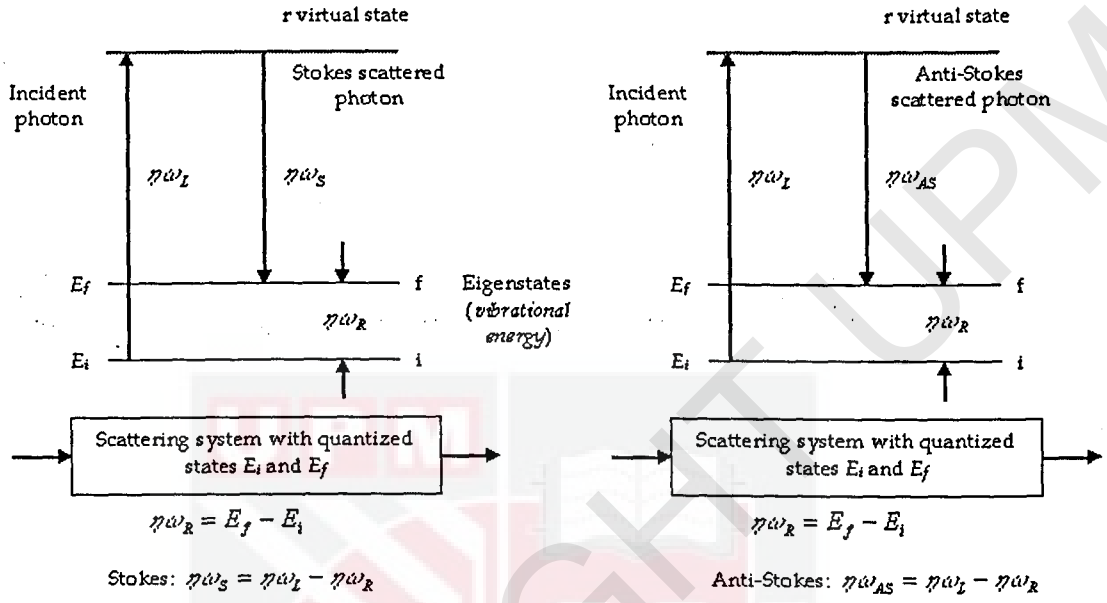

Figure 1.3: Simple model illustrating Stokes and Anti-Stokes Raman scattering.

The transition observed in Raman spectroscopy from molecules can be between rotational, vibrational or electronic eigenlevels. However, the observation of Raman scattering is in one case limited by the excitation of fluorescence, which is typically several orders of magnitude stronger than scattering. Raman scattering generally involves transitions amongst energy levels that are separated by much less than the photon energy of the incident light. The two level, denoted by E_0 and E_1 in **Figure 1.3**, for example, are most often vibrational levels, whilst the energies of the absorbed and emitted photons are commonly in (or near to) the visible range. Hence, the effect provides the facility for obtaining vibrational spectra using visible light.

The Raman Effect is the result of inelastic light scattering. A small amount of the photon energy of the incident light wave is modulated by the molecular scattering system. Nowadays only lasers of various wavelengths are used as light sources (Harris, 1996). An energy transfer occurs as a result of the coupling between the incident radiation and the quantized states of the scattering system. Depending on the coupling, the incident photons either gain or lose energy. Since only a small percentage of the incident energy is changed, most of the radiation will have the same frequency after the interaction. The latter is called elastically scattered light or Rayleigh scattering. The light, which has less energy compared to the incident laser light, is named Stokes-Raman scattering and the radiation which has larger energy is referred to as anti-Stokes-Raman scattering (Stephen *et al.*, 1975).

Raman scattering is the inelastic scattering of light by a material; the word 'inelastic' implies that energy is transferred between the light quanta and the material, so that the scattered light may have a longer or shorter wavelength than the incident light. The study of the spectrum of the light scattered from a particular material is, therefore, termed Raman spectroscopy and is of interest because, as will be seen, information can be gained about the structure, the composition and the vibration or electronic states of the scattering material.

1.9.4 Differential Thermogravimetric Analysis

Differential thermogravimetric analysis (DTA) is a thermoanalytic technique, similar to differential scanning calorimetry. In DTA, the material under study and an inert reference are made to undergo identical thermal cycles, while recording any temperature difference between sample and reference. This differential

temperature is then plotted against time, or against temperature (DTA curve or thermogram). Changes in the sample, either exothermic or endothermic, can be detected relative to the inert reference. Thus, a DTA curve provides data on the transformations that have occurred, such as glass transitions, crystallization, melting and sublimation. The area under a DTA peak is the enthalpy change and is not affected by the heat capacity of the sample.

The glass transformation occurs over a range of temperatures and cannot be characterized by any single temperature. However, it is convenient to be able to use just a single temperature as an indication of the onset of the glass transformation region during heating of a glass. This temperature, which is termed either the glass transformation temperature or the glass transition temperature (T_g), is rather vaguely defined by changes in either thermal analysis curves or thermal expansion curves. The values obtained from these two methods, while similar, are not identical. The value obtained for T_g is also a function of the heating rate used to produced these curves. Since T_g is a function of both experimental method used for the measurement and the heating rate used in the measurement, it cannot be considered to be a true property of the glass. However, T_g is a useful indicator of the approximate temperature where the supercooled liquid converts to a solid on cooling or conversely, of which the solid begins to behave as a viscoelastic solid on heating.

1.9.5 The Beer-Lambert's law

When UV-visible light beam of intensity I_0 strikes a sample, the intensity of light beam is reduced due to reflection and absorption in the sample

and, eventually, by scattering at dispersed particles. Before the development of adequate theory, Beer and Lambert had proposed laws of light absorption. Beer's Law states that the light absorbed by dilute solutions is proportional to the number of absorbing molecules or the concentration of absorbing molecules. On the other hand, Lambert's Law states that the fraction of radiation absorbed is independent to the intensity of radiation. These laws are well-known in their combined form as the Beer-Lambert law of light absorption which states that the fraction of the incident light absorbed is proportional to the number of molecules in the path. The intensity of an absorption band, i.e., the absorbance, is proportional to the number of absorbing species in the illuminated part of the sample. The absorbance for a material is the logarithm from the ratio of the intensities of the incident light and the transmitted light. Absorbance, A, is defined by the equation:

$$A = -\log T = \log\left(\frac{I_0}{I}\right) = dc\varepsilon \tag{1.7}$$

where I is the intensity of transmitted light, I_0 is the intensity of incident light, T is the transmittance of light, d is the thickness of a medium, c is conversion factor and ε is molar extinct coefficient of a medium.

Lambert's law, also called Bouguer's law or Lambert-Bouguer law, expresses the thickness effect of the absorbing medium on the absorption. If a homogenous medium is thought as constituted layers of uniform thickness normally to the beam, each layer absorbs the same fraction of

radiation incident on it. If I is the intensity to which a monochromatic parallel beam is attenuated after traversing a thickness d of the medium, and I_0 is the intensity of the beam at the surface incident (corrected for loss by reflection from the surface), the variation of intensity throughout the medium is expressed by:

$$I = I_0 e^{-\alpha d} \tag{1.8}$$

where α is a constant for medium called the absorption coefficient. The exponential relation can be expresses in an equivalent logarithmic form:

$$\log_{10}(I_0/I) = (\alpha/2.303)d = kd \tag{1.9}$$

where $k=\alpha/2.303$ is called the extinction coefficient for radiation of the wavelength considered. The quantity $log_{10}\ (I_0/I)$ is often called the optical density, or the absorbance of the medium.

1.9.6 Dielectric Theory

A solid material has electrical properties that can be characterized with resistivity, conductivity, permeability and others. For solid insulator material, this electrical property is known as dielectric property. Under the influence of alternating current field, it shows displacement of charges, especially bound charges in that material. This electrical property exist due to the material consist of charged atoms, where at times cancellation between positive charge and negative charge is not completed. Then there will exist electrical entity like dipole in the material. If alternating field is applied, every physics process exists is due to reaction between electrical field and electrical entity in the material will give permittivity property for each entity.

The reaction between these entities with applied electric field will produce inner electric field that gives effect to the permittivity of that material. Therefore permittivity shows the electrical process occurs in the dielectric material. By analyzing graph of permittivity against frequency, the main physical processes in the material that occurred can be determined. For low range frequency (less than 1 MHz), electrical entity in the material that has been detected is a dipole. The dipole exists whether in molecular form or due to motion of charges at the surface or at the grain boundary in the material and the motion of charges is not free or bound charge.

The electrical properties of materials as measured over a wide frequency range have been considerable interest subject in recent years. When some of the charge entity cannot move freely enough to follow immediately the variation of applied electric field, the displacement current acquires a component 90° out of phase with applied field and, the conduction component in phase with that field, the latter resulting in thermal dissipation of energy. Therefore the relative permittivity, ε_r is presented as complex permittivity,

$$\varepsilon^*(\omega) = \varepsilon'(\omega) - i\varepsilon''(\omega) \qquad (1.10)$$

where $\varepsilon'(\omega)$ is the relative permittivity for idealized polarization and $\varepsilon''(\omega)$ is associated with a conduction vector due to non ideality of the capacitor, known as relative loss factor. The permittivity of a material reflects the molecular relaxation and transport processes of the material which depend on many physical parameters such as temperature, time and pressure (Raju, 2003).

The expression relating the complex permittivity to the frequency is based on Debye which is given by

$$\varepsilon^*(\omega) = \varepsilon_\infty + \frac{\Delta\varepsilon}{1+i\omega/\omega_p} \tag{1.11}$$

the real and imaginary part of relative permittivity are given by

$$\varepsilon'(\omega) = \varepsilon_\infty + \frac{\Delta\varepsilon}{1+\left(\frac{\omega}{\omega_p}\right)^2} \tag{1.12a}$$

$$\varepsilon''(\omega) = \varepsilon_\infty + \frac{\Delta\varepsilon}{\left(\frac{\omega}{\omega_p}\right)^2+\left(\frac{\omega_p}{\omega}\right)^2} \tag{1.12b}$$

where $\Delta\varepsilon = \varepsilon_s - \varepsilon_\infty$ and ε_s is the static, low frequency permittivity, ε_∞ is the permittivity at the high frequency limit and $\omega_p = 2\pi f_p$is the frequency at which the maximum loss occur.

The Debye equation is suitable for presenting the dielectric data of liquids and gases. The behaviour of most dielectric material deviate in varying degree from the Debye equation and Cole-Cole modified the Debye equation by introducing a parameter, α. The Cole-Cole function can be written as

$$\varepsilon^*(\omega) = \varepsilon_\infty + \frac{\Delta\varepsilon}{1+(i\omega/\omega_p)^{1-\alpha}} \tag{1.13}$$

with

$$\varepsilon'(\omega) = \varepsilon_\infty + \frac{\Delta\varepsilon\left\{1+\left(\frac{\omega}{\omega_p}\right)^{1-\alpha}\sin\left(\alpha\frac{\pi}{2}\right)\right\}}{1+\left(\frac{\omega}{\omega_p}\right)^{2(1-\alpha)}+2\left(\frac{\omega}{\omega_p}\right)^{1-\alpha}\sin\left(\alpha\frac{\pi}{2}\right)} \tag{1.13a}$$

$$\varepsilon''(\omega) = \frac{\Delta\varepsilon\left(\frac{\omega}{\omega_p}\right)^{1-\alpha}\cos\left(\alpha\frac{\pi}{2}\right)}{1+\left(\frac{\omega}{\omega_p}\right)^{2(1-\alpha)}+2\left(\frac{\omega}{\omega_p}\right)^{1-\alpha}\sin\left(\alpha\frac{\pi}{2}\right)} \tag{1.13b}$$

where α is a parameter in the range between 0 and 1, still having symmetrical loss peak giving but broader than Debye function. Davidson and Cole later modified as to fit the experimental data and have the form:

$$\varepsilon^*(\omega) = \varepsilon_\infty + \frac{\Delta\varepsilon}{(1+i\omega\tau)^\beta} \tag{1.14}$$

with

$$\varepsilon'(\omega) = \varepsilon_\infty + \Delta\varepsilon(\cos\theta)^\beta \cos(\beta\theta) \tag{1.14a}$$

$$\varepsilon''(\omega) = \Delta\varepsilon(\cos\theta)^\beta \sin(\beta\theta) \tag{1.14b}$$

where β is a parameter in the range between 0 and 1, $\theta=tan^{-1}(\omega\tau)$ Havriliak and Negami proposed a generalization of the above equations which is given by

$$\varepsilon^*(\omega) = \varepsilon_\infty + \frac{\Delta\varepsilon}{\{1+(i\omega\tau)^{1-\alpha}\}^\beta} \quad ; \Delta\varepsilon = \varepsilon_s - \varepsilon_\infty \tag{1.15}$$

with

$$\varepsilon'(\omega) = \varepsilon_\infty + \frac{\Delta\varepsilon\cos(\beta\theta)}{r^{\beta/2}} \tag{1.15a}$$

$$\varepsilon''(\omega) = \frac{\Delta\varepsilon\sin(\beta\theta)}{r^{\beta/2}} \tag{1.15b}$$

where

$$r = \left[1 + (\omega\tau)^{1-\alpha}\sin\left(\frac{\alpha\pi}{2}\right)\right]^2 + \left[(\omega\tau)^{1-\alpha}\cos\left(\frac{\alpha\pi}{2}\right)\right]^2$$

$$\theta = arc\tan\left[\frac{(\omega\tau)^{1-\alpha}\cos\left(\frac{\alpha\pi}{2}\right)}{1+(\omega\tau)^{1-\alpha}\sin\left(\frac{\alpha\pi}{2}\right)}\right]$$

The parameters α and β in the above equations have no physical significance and were determined empirically. The Cole-Cole, Davidson-Cole and Havriliak-Negami functions are usually associated with a distribution of relaxation times. These empirical functions are suitable for fitting of experimental data and the best results can be achieved with two parameter Havriliak-Negami function.

Jonscher (1983) introduced the concept of power law (universal law) frequency respond of dielectric relaxation which was found suitable for fitting experimental data for a wide range of dielectric materials. According to the universal law, for

frequency above the loss peak, the dielectric response follows the equation of the form

$$\varepsilon'(\omega) \propto \varepsilon''(\omega) \propto \omega^{n-1} \tag{1.16}$$

with the exponent in the range $0 < n < 1$ and with the consequence that real and imaginary parts of the permittivity are in a frequency-independent ratio

$$\frac{\varepsilon''(\omega)}{\varepsilon'(\omega)} = \cot\left(\frac{n\pi}{2}\right) \tag{1.17}$$

is due to a mechanism for which the ratio of the energy lost per radian to the energy stored is frequency independent. That is

$$\frac{energy\ lost\ per\ radian}{energy\ stored} = \cot\left(\frac{n\pi}{2}\right) = constant \tag{1.18}$$

In the Debye form of relaxation, this ratio is equal to $\omega\tau$. Jonscher then proposes the following empirical relation for the loss factor as a function of frequency,

$$\varepsilon''(\omega) \propto \frac{1}{(\omega/\omega_p)^{-m} + (\omega/\omega_p)^{1-n}} \tag{1.19}$$

where ω_p is the loss peak frequency, with m and n are integers in the range 0 to 1. The term with exponent m dominates at frequency below the loss peak frequency, while the term with exponent 1-n dominates at frequency above the loss peak frequency. The real part of the permittivity ε' follows the relation

$$\varepsilon' \propto \begin{cases} \omega^{n-1} & for \quad \omega \gg \omega_p \\ constant & for \quad \omega \ll \omega_p \end{cases} \tag{1.20}$$

Based on the concept of universal law the experimentally observed behaviour for different dielectric dispersions have been explained with dipolar, quasi dc and diffusive mechanism (Hill and Pickup, 1985).

For bound dipolar, the fractional power law behaviour is given by

$$\varepsilon^*(\omega) \propto \varepsilon(0)\left(i\,\omega/\omega_p\right)^{n-1} \qquad \text{for} \quad \omega >> \omega_p$$

and $$\varepsilon(0) - \varepsilon^*(\omega) \propto \varepsilon(0)\left(i\,\omega/\omega_p\right)^{m} \qquad \text{for} \quad \omega << \omega_p \tag{1.21}$$

where $\omega_p = 2\pi f_p$ is the peak frequency, $\varepsilon(0)$ is the permittivity at very low frequency.

The quasi-dc process in which no loss peak is observed is characterized by two independent processes below and above certain critical frequency ω_c. In the quasi-dc process the real and imaginary parts of the permittivity increase steadily with decreasing frequency, with a small exponent at frequencies < ω_c is followed by a nearly flat loss behaviour above ω_c. The quasi-dc dispersion is represented by

$$\varepsilon^*(\omega) \propto \varepsilon(0)(i\,\omega/\omega_c)^{-p} \qquad \omega \ll \omega_c$$

and

$$\varepsilon^*(\omega) \propto \varepsilon(0)(i\,\omega/\omega_c)^{n-1} \qquad \omega \gg \omega_c \qquad (1.22)$$

The Dissado-Hill many body theory (Dissado and Hill 1982, Dissado *et al.*, 1987) assumes the cluster approach to the structure of condensed matter, and aims to explain the two independent processes in the dipolar response and quasi-dc processes in terms of intra-cluster and inter-cluster exchange mechanisms, above and below ω_p (for the dipolar process) or ω_c (for the quasi-dc process) respectively. Equivalent circuit modeling expression of quasi-dc behavior is reviewed in Appendix D.

Finally the dielectric response attributes to diffusions has been express as:

$$\varepsilon^*(\omega) \propto \varepsilon(\omega_d)(i\,\omega/\omega_d)^{-s} \qquad s \cong 0.5 \qquad (1.23)$$

Ngai and White (1979), Ngai (1981), and Dissado and Hill (1979) have developed theories due to the interaction effects with different approaches. It has been shown (Niklasson, 1989) that the most better and advance model is proposed by Dissado and Hill (1983) based on the concept of many body theory. Dissado and Hill

explained the mechanism response in terms of cooperation between clusters. The parameters used in the Cole-Cole, Davidson-Cole, and Havrilak-Negami functions have no physical significance, and the value has been determined by empirical means. On the other hand, the exponent n-1 used in the universal law has the physical significance regarding the degree of ordering in the system, based on the experimental observation. The summary of the dielectric spectra response is tabulated in **Table 1.1.**

Table 1.1: The summary of various spectral functions and their power law exponents [Hill and Jonscher, 1983].

Process	Susceptibility function	exponent for $\omega \ll \omega_p$		exponent for $\omega \gg \omega_p$	
		$\Delta\chi''(\omega)$	$\chi''(\omega)$	$\chi''(\omega)$	$\chi''(\omega)$
One parameter					
Debye	$(1+i\omega/\omega_p)^{-1}$	2.0	1.0	-2.0	-1.0
Cole-Cole (1941)	$\left(1+\left(i\omega/\omega_p\right)^{1-\alpha}\right)^{-1}$	1-α	1-α	1-α	α-1
Fuoss-Kirkwood (1941)	$2\left(\omega/\omega_p\right)^{\gamma}\left(1+\left(\omega/\omega_p\right)^{2\gamma}\right)^{-1}$	γ	γ	-γ	-γ
Davidson-Cole (1951)	$\left(1+i\omega/\omega_p\right)^{-\beta}$	3.0	1.0	-β	-β
Williams-Watts (1970)	$\sum_{s=1}^{\infty}\frac{\Gamma(\Delta s)}{(s-1)!}\left\lvert\frac{\exp(-i\Delta\pi/2)}{\omega^{\Delta}\omega_p^{-\Delta}}\right\rvert^{s}$	2.0	1.0	-Δ	-Δ
Two parameter					
Havrilak-Negami (1966)	$\left(1+\left(i\omega/\omega_p\right)^{1-\alpha}\right)^{-\beta}$	1-α	1-α	-β(1-α)	-β(1-α)
Jonscher (1975)	$\left(\omega/\omega_1\right)^{-m}+\left(\omega/\omega_2\right)^{1-n}\Big)^{-1}$	m	m	n-1	n-1
Hill (1978)	$\omega^{m}\left(\omega_p^{2s}+\omega^{2s}\right)^{-(m+1-n)/2s}$	m	m	n-1	n-1
Dissado-Hill (1979)	$\left(1+i\omega/\omega_p\right)^{n-1}\times{}_2F_1\left(1-n,1-m;2-n;\frac{\omega_p}{\omega_p+i\omega}\right)$	m	m	n-1	n-1

*All the spectral parameter α, β, Δ, γ, m and n are fractional and positive.
† The Fuoss-Kirkwood relationship gives only the imaginary component $\chi''(\omega)$.

In general, polarizations have four different dielectric mechanisms (**Figure 1.4**). The four types of polarization mechanism (**Figure 1.5**) that is occurring in solid-state materials are (Moulson and Herbert, 1987):

1. Space charge polarization: Occurs when more than one material component is present or when segregation occurs in a material containing incompatible

chemical sequences and when translating charge carriers become trapped at the interfaces of heterogeneous systems. This type of polarization occurs in the range of 10^{-2} to 10^{4} Hz.

2. Dipole polarization: Unbalanced sharing of electrons causes a permanent dipole moment by atoms of a molecule. In an absence of an external electric field, these moments are oriented in a random order such that no net polarization is present. Under an external electric field, the dipoles rotate to align with the electric field causing orientation polarization to occur and happened in microwave frequency in the range of 10^{3} to 10^{8} Hz.
3. Ionic polarization: Occurs when neighbouring positive and negative ions "stretch" under an applied electric field. This polarization only happens in the infrared region (10^{12} to 10^{13} Hz).
4. Electronic polarization: Occurs in neutral atoms when an electric field displaces the nucleus with respect to the electrons that surround it. The positive charge in the nucleus and the centre of the negative charges from the electron "cloud" will thus experience forces in different direction and will become separated due to the force of the field direction. It happens only at high frequency in the ultra violet range (10^{14} to 10^{16} Hz).

The permittivity of a medium containing several possible fast respond polarization mechanisms (induced atomic or electronic and ionic lattice) which contribute a purely real value, ε_{∞} and the slower responses; permanent molecular dipole, ionic defects of dipolar type (vacancy-interstitial pairs) and also slowly mobile hopping charge carriers of electronic, polaronic or ionic nature.

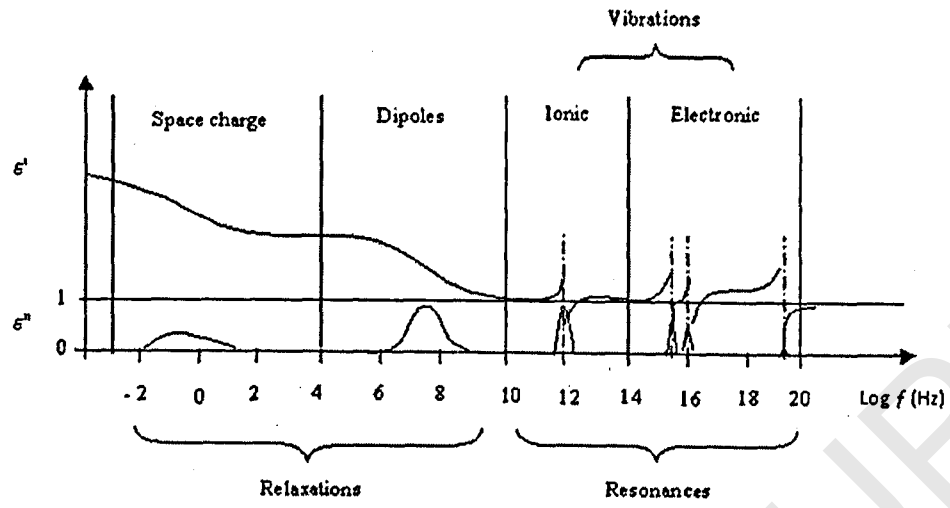

Figure 1.4: The various types of interaction between the electromagnetic field and matter and the relevant relative permittivity (Raju, 2003).

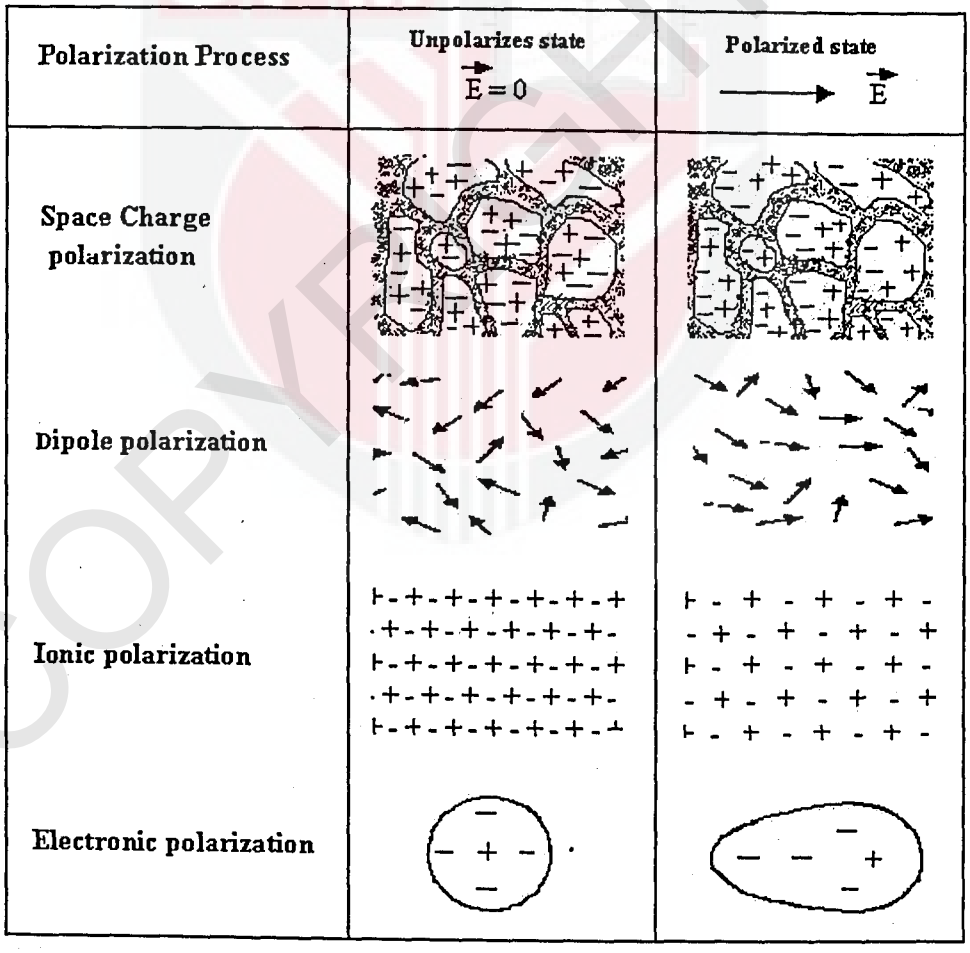

Figure 1.5: The polarization process with no electric field and with applied electric field (Moulson and Herbert, 1987).

1.10 Outline of the thesis

The first chapter gives research overview, problem statement, significant of study and objectives of author's work. In Chapter 2, a brief literature review has been made for density, differential thermal analysis (DTA), optical absorption spectra, Raman spectra, dielectric properties of lead borotellurite glass system. On the other hand, an outline of the experimental techniques and relevant system employed is given in Chapter 3. Obviously, Chapter 4 deals with the discussion of the experimental results obtained from author's study for density, differential thermal analysis (DTA), XRD, optical absorption spectra, Raman spectra and dielectric mechanism of lead borotellurite glass system. Not only theories of radiation and Raman will be discussed in this chapter but the theories of thermal stability, optics and dielectric will also be presented in this chapter. To sum up, general conclusions and suggestions for future work will be given in Chapter 5.

BIBLIOGRAPHY

Al-Ani, S. K. J., Hogarth, C. A., El-Malawany, R. A., 1985. A study of optical absorption in tellurite and tungsten-tellurite glasses. *Journal of Materials Science* 30: 3720-3729.

Arnaudov, M., Dlmlzrov, V., Dimitriev, Y., Markova, L., 1982. Infrared-spectral investigation of tellurites. *Material Research Bulletin* 17: 1121-1129.

Balboul, M. R., 2008. Optical effects induced by gamma and UV irradiation in chalcogenic glass. *Radiation Measurements* 43: 1360-1364.

Charton, P., Thomas, P., Armand, P., 2003. Raman and crystallization behaviors of TeO_2–Sb_2O_4 glasses. *Journal of Non-Crystalline Solids* 321: 81-88.

Chen, G., Baccaro, S., Cecelia, A., Youguan Du, Mihokova, E., Nikl, M., Nitsch, K., 2001. How cerium affect irradiation resistance. *American Ceramic Society Bulletin* 80 (4): 107-109.

Cheng, Yin, Xiao, Hanning, Guo, Weiming, 2007a. Influence of compositions on sealing temperature and properties of lead borate non-crystallizing sealing glasses. *Materials Science and Engineering A* 464: 210-215.

Cheng, Yin, Xiao, Hanning, Guo, Weiming, 2007b. Structure and crystallization kinetics of PbO–B_2O_3 glasses. *Ceramics International* 33: 1341-1347.

da Rocha, M.S.F., Pontuschka, W.M. Blak, A.R., 2003. Radation induced capacitance in barium aluminoborate glasses. *Journal of Non-Crystalline Solids* 321: 29-36.

Davisson, C.M. and Evans, R., 1952. Gamma-ray Absorption Coefficients *Review of Modern Physics*, 24: 79-107.

Dissado, L. A. and Hill, R. M., 1979. Non-exponential decay in dielectric and dynamics of correlated systems. *Nature* 279: 685-689.

Dissado, L. A. and Hill, R. M., 1982. Examination of the dielectric susceptibility of poly(γ-Benzyl-L-glutamate). *Journal of Chemistry Society Faraday Trans.*, 2(78): 81-93.

Dissado, L. A. and Hill, R. M., 1983. A cluster approach to the structure of imperfect materials and their relaxation spectroscopy. *Progress of Royal Socity London A* 390: 131-180.

Dissado, L. A., Rowe, R. C., Haider, A, Hill, R. M., 1987. The characterization of heterogeneous gels by means of a dielectric technique. I- Theory and preliminary evolution. *Journal of Colloid and Interface Science*, 117(2): 310-324

Dollish, Fateley, Bentley., *Characteristic Raman Frequencies of Organic Compounds*, John Wiley & Sons Publication: Canada, 1974.

El Batal, Fatma H., 2007. Gamma ray interaction with bismuth silicate glasses. *Nuclear Instruments and Methods in Physics Research B* 254: 243-253.

El Batal, Fatma H., Ashour, Ahmed H., 2002. Effect of gamma irradiation on the electrical conductivity of ternary borate glasses. *Materials Chemistry and Physics* 77: 677-686.

El-Alaily, N. A., Mohamed, R. M., 2003. Effect of irradiation on some optical properties and density of lithium borate glass. *Materials Science and Engineering B* 98: 193-203.

El-Deen, L. M. Sharaf, Al-Salhi, M. S., Elkholy, M. M., 2008. Radiation induced color centers in $50PbO–50P_2O_5$ glass. *Journal of Non-Crystalline Solids* 354: 5453-5458.

El-Mallawany, R., El-Sayed, Adly H., El-Gawad, M.M.H. Abd, 1995. ESR and electrical conductivity studies of $(TeO_2)_{0.95}$ $(CeO_2)_{0.05}$ semiconducting glasses. *Materials Chemistry and Physics* 41: 87-91.

El-Moneim, Abd A., 2002. DTA and IR absorption spectra of vanadium tellurite glasses, *Materials Science Communication*. 73: 318-322.

Ezz-Eldin, F. M., 1999. Radiation effects on some physical and thermal properties of V_2O_5-P_2O_5 glasses. *Nuclear Instruments and Methods in Physics Research B* 159: 166-175.

Ezz-Eldin, F. M., Elalaily, N. A., El-Batal H. A., and Ghoneim, N. A., 1996. Formation and bleaching of induced colour centres in gamma-irradiated vanadium-containing alkali-borate glasses. *Radiation Physics Chemistry* 48: 659-664.

Fanderlik, Ivan, *Optical properties of glass: Glass science and technology 5*. Elsevier: Amsterdam – Oxford – New York - Tokyo, 1983.

Fouad, S. S., El-Shazly, E. A. A., Balboul, M. R., Fayek, S. A., El-Bana, M. S., 2006. Optical parameter studies of thermally evaporated As-Se-Sn glassy system. *Journal of Materials Science* 17: 193-198.

Fuxi, Gan, *Optical and spectroscopic properties of glass*, Springer-Verlag: Berlin – Heidelberg – New York and Shanghai Scientific and Technical Publishers, 1992.

Gerhardt, R., 1994. Impedance and dielectric spectroscopy revisited: Distinguishing localized relaxation from long-range conductivity. *Journal of Physics and Chemistry Solids* 55(12): 1491-1506.

Gopi Sharma, Kulwant Singha, Manupriya, Shaweta Mohan, Harvinder Singh, Sukhleen Bindra. 2006 Effects of gamma irradiation on optical and structural properties of $PbO–Bi_2O_3–B_2O_3$ glasses. *Radiation Physics and Chemistry*. 75: 959-966.

Halimah, M. K, Daud, W. M., Sidek, H. A. A., Zainul, H., Zainal, A. T., Zainul, H. and Jumiah Hassan, 2005. Optical Properties of Borotellurite Glasses. *American Journal of Applied Sciences* Special Issue: 63-66.

Harris, D.A., *Light Spectoscopy: Introduction to Biotechniques* Bios Scientific Publisher: UK, 1996.

Harvinder Singh, Kulwant Singh, Leif Gerward, Kanwarjit Singh, Hari Singh Sahota, Rohila Nathuram, 2003. $ZnO–PbO–B_2O_3$ glasses as gamma-ray shielding materials. *Nuclear Instruments and Methods in Physics Research B* 207: 257-262.

Hideharu Ushida, Yasuhiko Iwadate, Takeo Hattori, Shin Nishiyama, Kazuko Fukushima, Yasuhisa Ikeda, Makoto Yamaguchi, Masakatsu Misawa, Toshiharu Fukunaga, Tetsuya Nakazawa, Shiro Jitsukawa, 2004. Network structure of $B_2O_3–PbO$ and $B_2O_3–PbO–PbBr_2$ glasses analyzed by pulsed neutron diffraction and Raman spectroscopy. *Journal of Alloys and Compounds* 377: 167-173.

Hill, R. M. and Pickup, C., 1985. Barrier effect in dispersive media. *Journal of Material Science*, 20: 4431-4444.

Hogarth, C. and Kashani, E., 1983. Some studies of the optical properties of tungsten-calcium-tellurite glasses. *Journal of Materials Science*, 18: 1255-1263.

Hoppe, U., 1999. Behavior of the packing densities of alkali germanate glasses. *Journal of Non-Crystalline Solids* 248: 11-18.

Jonscher, A. K., *Dielectric relaxation in solid.* Chelsea Dielectrics Press: London, 1983.

Joseph B. Lambert, Herbert F. Shurvell, Lawrence Verbit, R. Graham Cooks, *Organic Structural Analysis*, Macmillan Publishing Co., Inc.: New York, 1978.

Jung, Byung-Hae, Kim, Hyung-Sun, 2004. Influence of Nd_2O_3 on the thermal and dielectric properties of Pb-based lead borosilicate glasses. *Journal of Non-Crystalline Solids* 336: 96-101.

Kaur, Arshpreet, Khanna, Atul, Pesquera, Carmen, González, Fernando, Sathe, Vasant, 2010. Preparation and characterization of lead and zinc tellurite glasses. *Journal of Non-Crystalline Solids* 356: Issues 18-19, 864-872.

Khanna, A., Bhatti, S.S., Singh, K.J., Thind, K.S. 1996. Gamma-ray attenuation coefficients in some heavy metal oxide borate glasses at 662 keV, *Nuclear Instruments and Methods in Physics Research Section B: Beam Interactions with Materials and Atoms*. 114, Issues 3-4: 217-220.

Khatir, S., Romain, F., Portier, J., Rossignol, S., Tanguy, B., Videau, J. J., Turrell, S., 1993. Raman studies of recrystallized glasses in the binary TeO_2-PbO system. *Journal of Molecular Structure* 298: 13-16.

Kneipp, K., Burger, H., Fassler, D., and Vogel, W., 1984. Raman spectroscopic study on glasses in the system K_2O-B_2O_3-TeO_2. *Journal of Non-Crystalline Solids* 65: 223-232.

Kutub, A. A., Elmanhawaawy, M. S. and Shawoosh, A. S., 1996. Optical Properties of γ-irradiated Sodium Diborate Glasses Containing Copper and Cerium. *Physics State Solid* 155: 239-248.

Macdonald, J. Ross, *Impedance spectroscopy: Emphasizing solid materials and system*. John Wiley & Sons: New York – Chichester – Brisbane – Toronto – Singapore, 1987.

Malik, M. Suleman and Hogarth, C. A., 1990. Effect of cobalt oxide on the a.c. conduction mechanism of copper tellurite glasses. *Journal of Materials Science* 25: 3208-3214.

McLaughlin, W.L., Boyd, A.W., Chadwick, K.H., McDonal, J.C. and Miller, A., *Dosimetry for Radation Processing*, Taylor & Francis, 1995.

McLaughlin, W.L., *Radioactivity Measurements: Principles and practice*, Pergamon Press: Great Britain,1988.

Moguš-Milanković, A., Šantić, A., Reis, S.T., Furić, K., Day D.E., 2005. Studies of lead–iron phosphate glasses by Raman, Mössbauer and impedance spectroscopy. *Journal of Non-Crystalline Solids* 351: 3246-3258.

Mohamed, Tarek A., Shaltout, I., Al Yahyae, K. M., 2006. Structural characterization of tellurite glasses doped with transition metal oxides using Raman spectra and ab initio calculations. *Spectrochimica Acta Part A* 64: 106-115.

Mott, N. F. and Davis, E. A., *Electronic Processes in Non-crystalline Materials*. Oxford: Clarendon Press, 1979.

Mott, N. F., 1993. Superconductivity in chalcogenide glasses. *Journal of Non-Crystalline Solids* 164-166: 1177-1178.

Moulson, A. J. and Herbert, J. M., *Electroceramics*, London: Chapman and Hall, 1987.

Ngai, K. L. and White, C. T., 1979. Frequency dependence of dielectric loss in condensed matter. *Journal of Physical review B* 20: 2475-2486.

Ngai, K. L., 1981. The universal low frequency responses of ionic conductor: A review of data and a unified model interpretation. *Journal of Solid State Ionic* 5: 27-34.

Niklasson, G. A., 1989. Comparison of dielectric response functions for conducting materials. *Journal of Apply Physics* 66: 4350-4359.

Pan, Zhengda, Morgan, Steve H., 1997. Raman spectra and thermal analysis of a new lead-tellurium-germanate glass system. *Journal of Non-Crystalline Solids* 210: 130-135.

Perkins, D. H. *Introduction to high energy physics*. Addison Wesley: London, 1987.

Piao, F., Oldham, W.G., Haller, E.E., 2000a. The mechanism of radiation-induced compaction in vitreous silica. *Journal of Non-Crystalline Solids* 276: 61-71.

Piao, F., Oldham, W.G., Haller, E.E., 2000b. Ultraviolet-induced densification of fused silica *Journal of Applied Physics* 87(3): 3287.

Prashant Kumar, M., Sankarappa, T., Vijaya Kumar, B., Nagaraja, N., 2009. Dielectric relaxation studies in transition metal ions doped tellurite glasses. *Solid State Sciences* 11: 214-218.

Rachkovskaya, G. E. and Zakharevich, G. B., 2002. Vitrification, properties, and structure of lead-tellurite borate glasses. *Glass and Ceramics* 59: 3 – 4.

Rachkovskaya, G. E. and Zakharevich, G. B., 2004. Properties, structure, and application of low-melting lead–bismuth glasses. *Glass and Ceramics* 61: 1 – 2.

Raju, Gorur G., *Dielectrics in electric fields*. Marcel Dekker Inc., 2003.

Ravi Kumar, V., and Veeraiah, N., 1998. Dielectric properties of ZnF_2-PbO-TeO_2 glasses. *Journal of Physics, Chemistry and Solid* 59: 91-97.

Rawson, H. *Inorganic glass-forming systems*. Academic Press: London, 1967.

Rawson, H. *Properties and applications of glass: Glass science and technology 3*. Elsevier: Amsterdam – Oxford – New York, 1980.

Rivero, Clara, Richardson, Kathleen, Stegeman, Robert, Stegeman, George, Cardinal, Thierry, Fargin, Evelyne, Couzi, Michel, Rodriguez, Vincent, 2004. Quantifying Raman gain coefficients in tellurite glasses. *Journal of Non-Crystalline Solids* 345 & 346: 396-401.

Roger, J. Berry and Niels, W. Holm, Introduction to Basic Concepts and Principle in Radiation in *Dosimetry Manual on Radiation Dosimetry*, Marcel Dekker Inc.: New York 1970, pp 4-6.

Rong, Qiu Jian, Osaka, Akiyoshi, Nanba, Tokuro, Takada, Jun, Miura, Yoshinari, 1992. Infrared and Raman spectra of binary tellurite glasses containing boron and indium oxides. *Journal of Materials Science* 27: 3793-3798.

Runt, James P. and Fitzgerald, John J., *Dielectric spectroscopy of polymeric materials: fundamentals and applications*. American Chemical Society: Washington USA, 1997.

Sabry, A. I., and El-Samanoudy, M. M., 1995. Optical, infrared and electrical conductivity of glasses in the TeO_2-B_2O_3 system. *Journal of Materials Science* 30: 3930-3935.

Saddeek, Yasser B., 2004. Ultrasonic study and physical properties of some borate glasses. *Materials Chemistry and Physics* 83: 222-228.

Saddeek, Yasser B., 2009. Structural and acoustical studies of lead sodium borate glasses. *Journal of Alloys and Compounds* 467: 14-21.

Sekiya, Takao, Mochida, Norio, Ogawa, Shinji, 1994. Structural study of WO_3-TeO_2 glasses. *Journal of Non-Crystalline Solids* 176: 105-115.

Sekiya, Takao, Mochida, Norio, Ohtsuka, Atsushi and Soejima, Ayako, 1992. Raman spectra of $BO_{3/2}$-TeO_2 glasses. *Journal of Non-Crystalline Solids* 151: 222-228.

Shaltout, I., Tang, Yi, Braunsteint R., and Shaishas, E. E., 1996. FTIR spectra and some optical properties of tungstate-tellurite glasses. *Journal of Physics and Chemistry of Solids* 57: 1223-1230.

Sharma, G., Thind, K. S., Manupriya, Klare, H. S., Narang, S. B., Gerward, L., Dangwal, V. K., 2006. Effects of gamma-ray irradiation on optical properties of ZnO–PbO–B_2O_3 glasses. *Nuclear Instruments and Methods in Physics Research B* 243: 345-348.

Sharma, M. V. N. V. D., Sarma, A. V., Rao, R. Balaji, 2009. Electrical Characterization and Relaxation Behavior of Lithium-Indium-Phosphate Glasses via Impedance Spectroscopy *Turkey Journal of Physics* 33: 87-100.

Shelby, James E. *Introduction to glass science and technology*. Second Edition: The Royal Society of Chemistry: U.K., 2005.

Sheoran, A., Sanghi, S., Rani, S., Agarwal, A., Seth, V.P., 2009. Impedance spectroscopy and dielectric relaxation in alkali tungsten borate glasses. *Journal of Alloys and Compounds* 475: 804-809.

Shpotyuk, I. O., Balitska, V. O., Vakiv, M. M., Shpotyuk, L. I., 1998. Sensors of high-energy radiation based on amorphous chalcogenides. *Sensors Actuator A* 68: 356-358.

Sidek, H. A. A., Hamezan, M., Zaidan, A. W., Talib, Z. A., and Kaida, K., 2005. Optical Characterization of Lead-Bismuth Phosphate Glasses. *American Journal of Applied Sciences* 2(8): 1266-1269.

Silva, M. A. P., Messaddeq, Y., Ribeiro, S. J. L., Poulain, M., Villain, F., Briois, V., 2001. Structural studies on TeO_2±PbO glasses. *Journal of Physics and Chemistry of Solids* 62: 1055-1060.

Sokolov, V. O., Plotnichenko, V. G., Koltashev, V. V., Dianov, E. M., 2006. On the structure of tungstate–tellurite glasses. *Journal of Non-Crystalline Solids* 352: 5618-5632.

Stephen E. Wiberly, Lawrence H. Daly, Norman B. Colthup, *Introduction to Infrared and Raman Spectroscopy*, Academic Press: New York, 1975.

Subbalakshmi, P., Veeraiah, N., 2002. Dielectric dispersion and certain other physical properties of PbO–Ga_2O_3–P_2O_5 glass system. *Materials Letters* 56: 880-888.

Syam Prasad, P., Raghavaiah, B.V., Balaji Rao, R, Laxmikanth, C., Veeraiah, N, 204. Dielectric dispersion in the PbO-MoO_3-B_2O_3 glass system. *Solid state Communications* 132: 235-240.

Tauc, J., *Amorphous and lliquid semiconductors*, Plenum Publishing Company Ltd.: London, 1974.

Tikhomirov, V. K., Jha, A., Perakis, A., Sarantopoulou, E., Naftaly, M., Krasteva, V., Li, R., Seddon, A. B., 1999. An interpretation of the Boson peak in rare-earth ion doped glasses. *Journal of Non-Crystalline Solids* 256 & 257: 89-94.

Upender, G., Sathe, Vasant G., Chandra Mouli, V., 2010. Raman spectroscopic characterization of tellurite glasses containing heavy metal oxides. *Physica B* 405: 1269-1273.

Varshneya, A. K., Fundamentals of Inorganic Glasses. Academic Press: New York, 1994.

Veerabhadra Rao, A., Laxmikanth, C., Appa Rao, B., Veeraiah, N., 2006. Dielectric relaxation and a.c. conduction phenomena of $PbO–PbF_2–B_2O_3$ glasses doped with FeO. *Journal of Physics and Chemistry of Solids* 67: 2263-2274.

Załuski, L. and Trykozko, R., 1981. Electrical resistivity of Te-Ge-Pb glasses. *Solid State Communications* 37: 527-528.

Zhang, Junjie, Qiu, Jianbei, Kawamoto, Yoji, 2002. New oxyfluorotellurite glass: thermal analysis and structural analysis by means of Raman scattering. *Materials Letters* 55: 77-82.